Supporting Information

Characteristics of Ag-doped $LaMnO_3$ perovskite oxide and its application as a solid oxide fuel cell cathode

Characteristics of Ag-doped $LaMnO_3$ perovskite oxide and its application as a solid oxide fuel cell cathode

Akihiro Takamatsu,[a] Masatsugu Oishi,[a,*] Shinpei Goda,[a] Hiroki Takemura,[a] Konosuke Mitsushio,[a] Satoshi Sugano,[a] Takashi Yamamoto,[a] Toshiaki Ina,[b] Haruo Kishimoto,[c] and Takaaki Sakai,[c,**]

[a]Graduate School of Technology, Industrial and Social Science, Tokushima University, 2-1 Minami Josanjima Cho, Tokushima 770-8506, Japan
[b]Japan Synchrotron Radiation Research Institute (JASRI), 1–1–1 Kouto, Sayo-cho, Sayo-gun, Hyogo 679–5198, Japan
[c]National Institute of Advanced Industrial Science and Technology (AIST), Global Zero Emission Research Center, 16-1 Onogawa, Tsukuba, Ibaraki 305-8569, Japan

* Corresponding author: Dr. Masatsugu Oishi
Graduate School of Technology, Industrial and Social Science, Tokushima University, 2-1 Minami Josanjima Cho, Tokushima 770-8506, Japan
Tel: +81-88-656-7367
E-mail: ooishi.masatsugu@tokushima-u.ac.jp

** Corresponding author: Dr. Takaaki Sakai
National Institute of Advanced Industrial Science and Technology (AIST), Global Zero Emission Research Center,16-1 Onogawa, Tsukuba, Ibaraki 305-8569, Japan
Tel: +81-29-861-8212
E-mail: sakai-takaaki@aist.go.jp

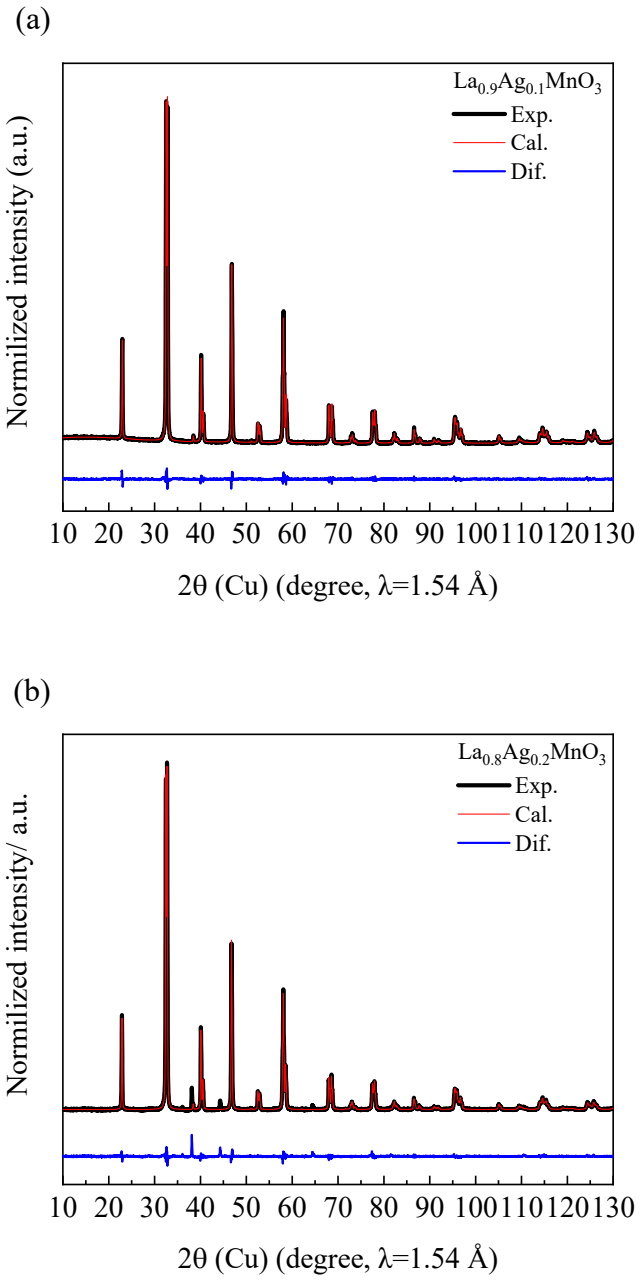

Figure S1 Rietveld refinements of the XRD pattern of (a) $La_{0.9}Ag_{0.1}MnO_3$ and (b) $La_{0.8}Ag_{0.2}MnO_3$.

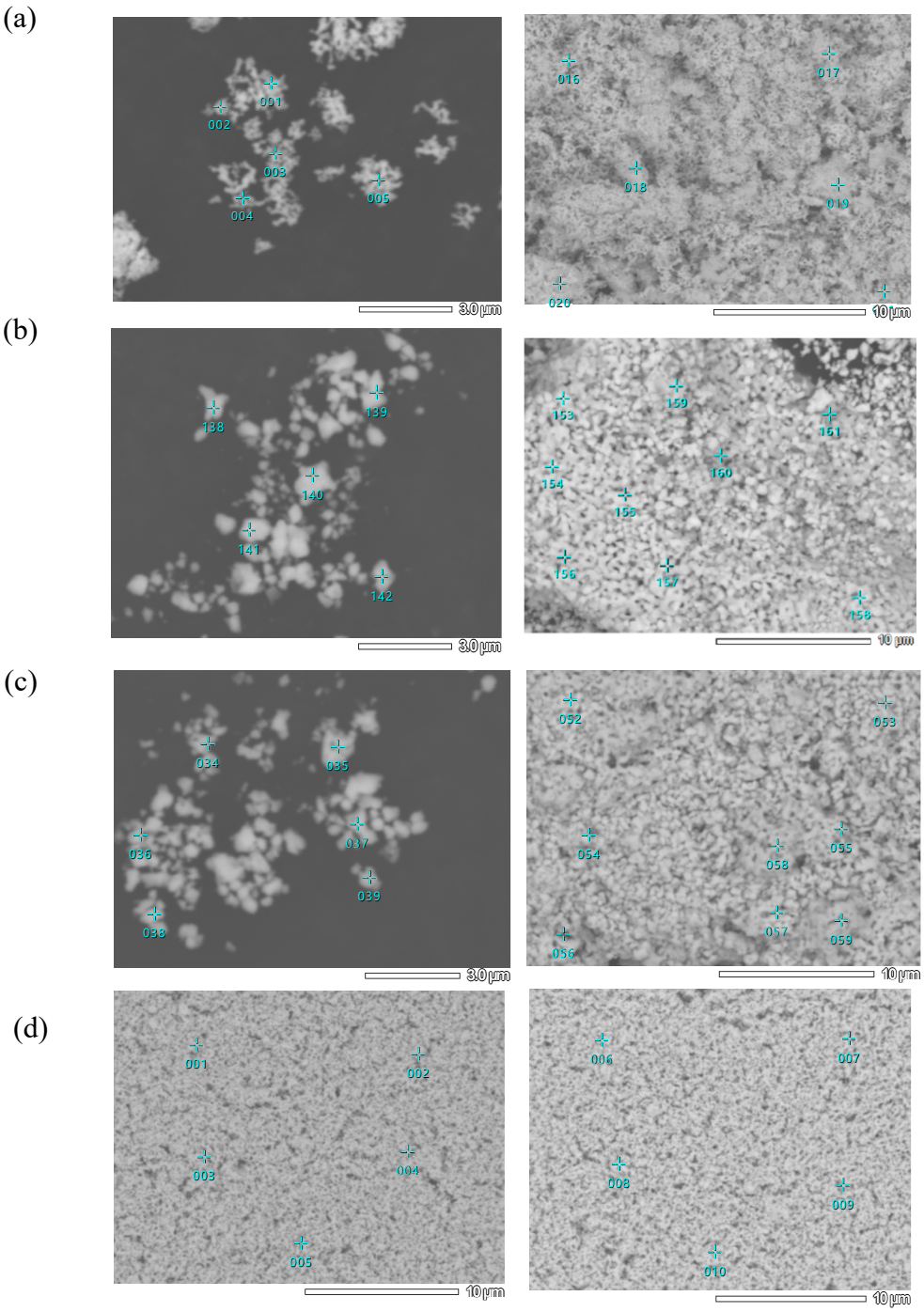

Figure S2 Typical SEM images used for the EDX elemental analyses of (a) LAM01 pristine powders, (b) LAM01 powders annealed at 975 °C for 100 h, (c) LAM01 cathode (baked at 1000 °C) after the power generation tests, and (d) LAM01 cathode (baked at 925 °C) after the power generation tests.

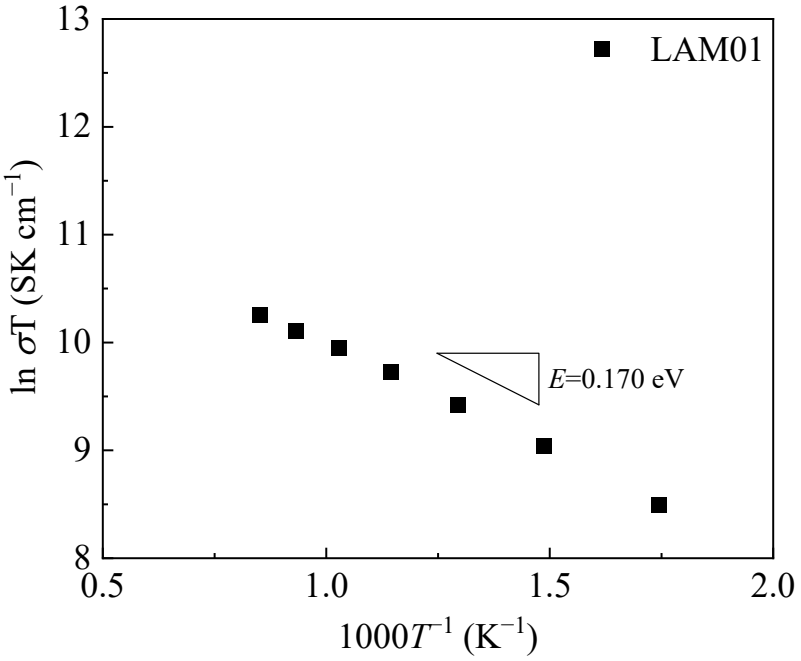

Figure S3 Plots of ln(σT) of the electrical conductivity of LAM01 against T^{-1}.

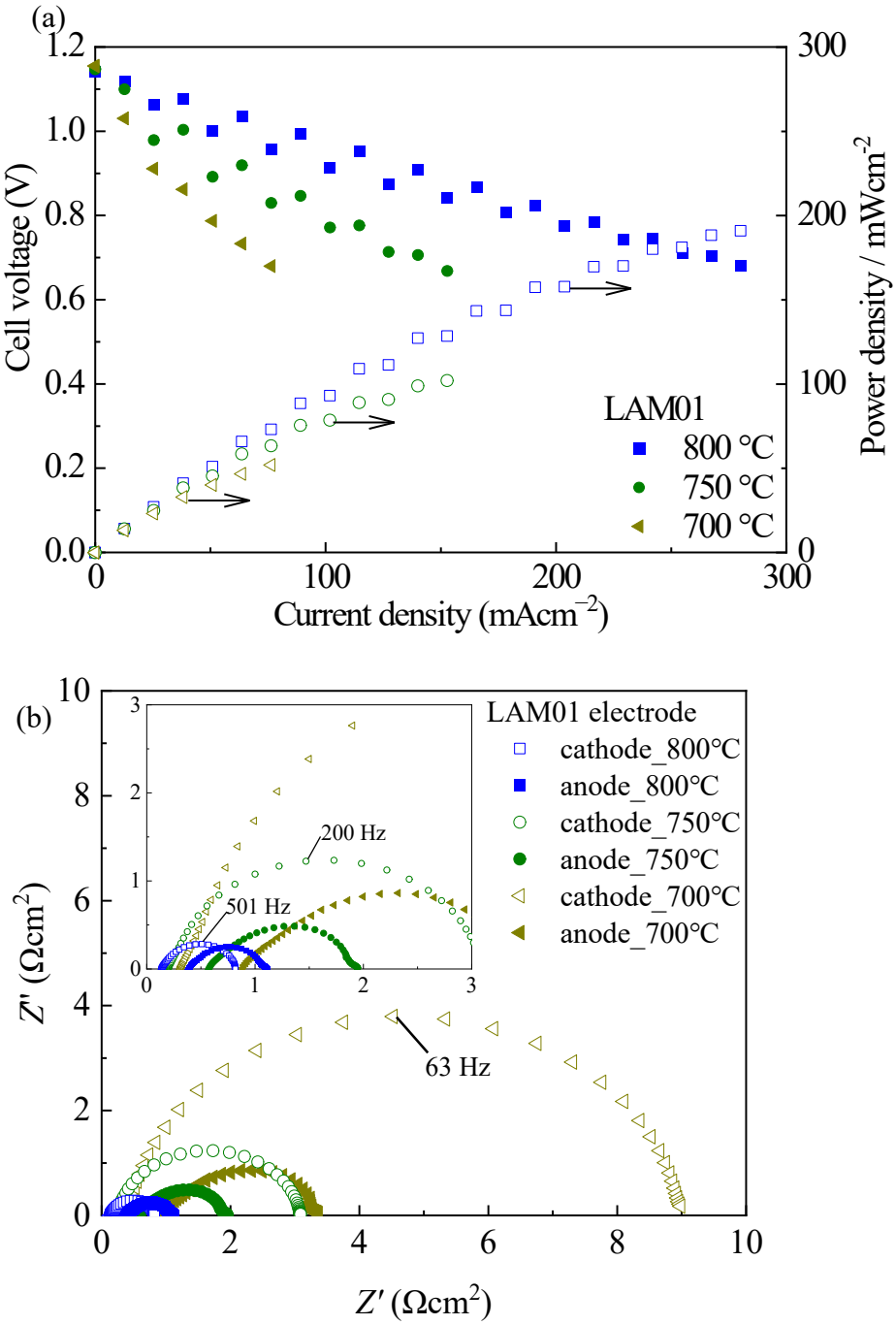

Figure S4 (a) Power generation characteristics curve and (b) impedance profiles of the LAM01 cathode cell. The cathode was baked at 1000 °C.

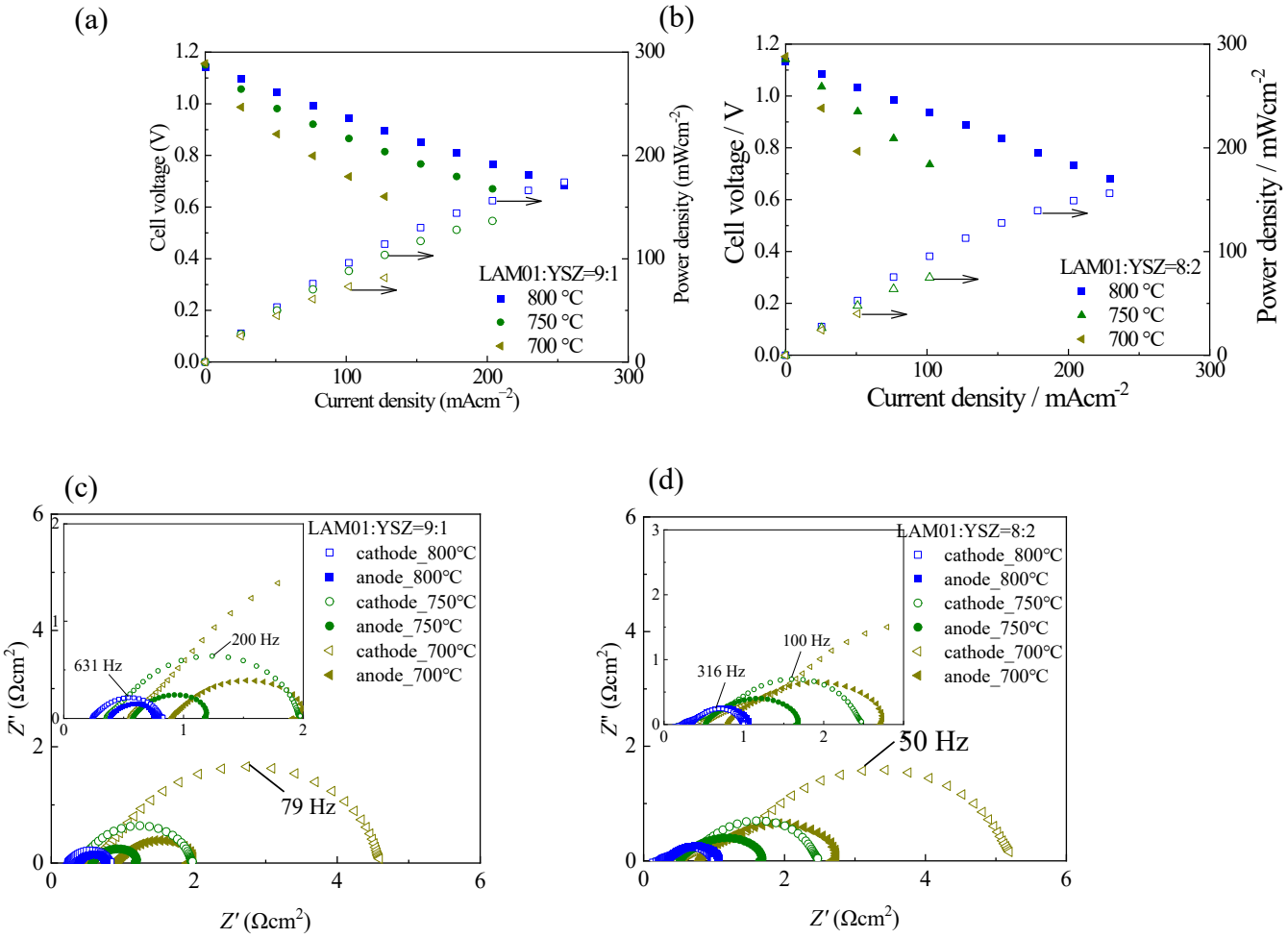

Figure S5 Power generation characteristics curves of the (a) LAM01+YSZ (9:1) composite cathode cell and (b) LAM01+YSZ (8:2) composite cathode cell. Complex impedance plots of the (c) LAM01+YSZ (9:1) cathode cell and (d) LAM01+YSZ (8:2) cermet cathode cell. The cathode was baked at 1000 °C.

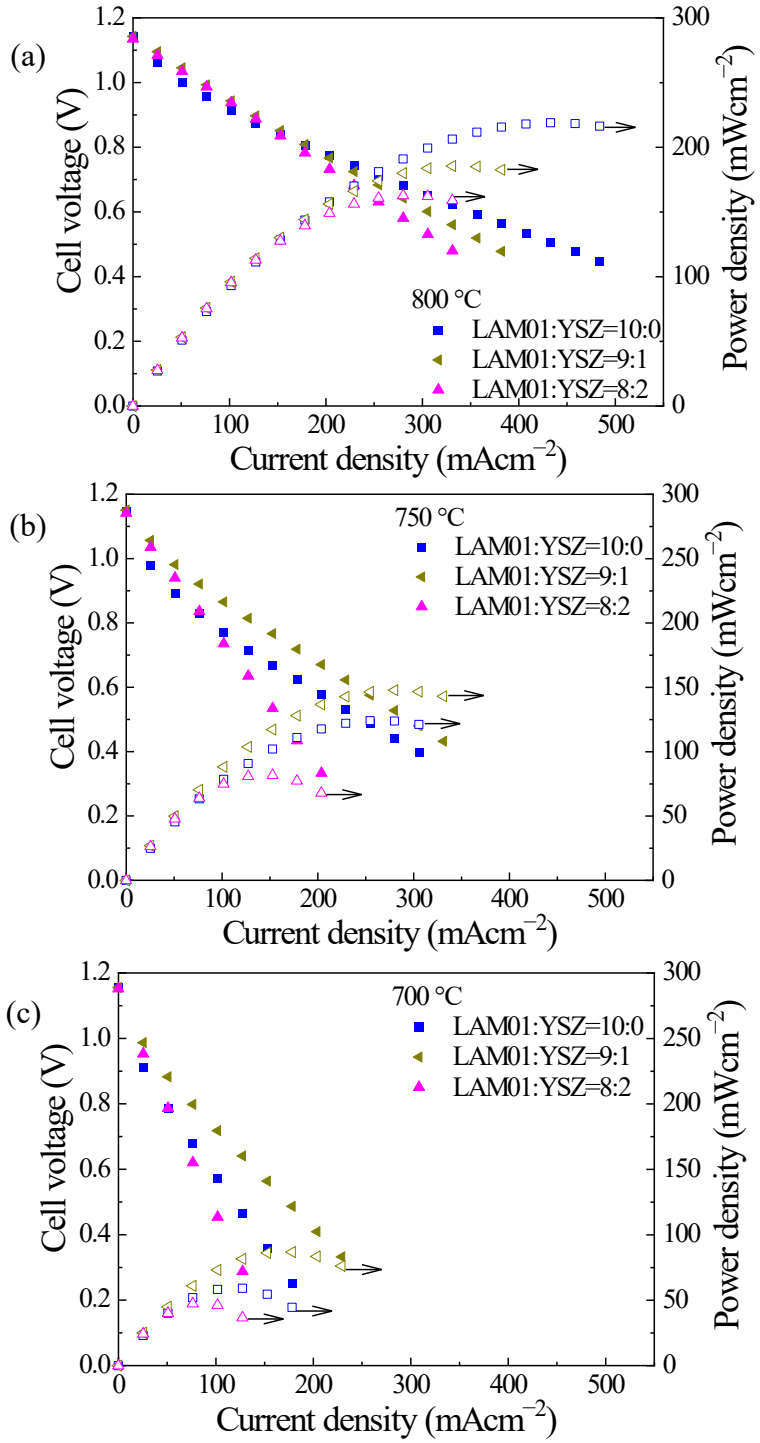

Figure S6 Comparison of power generation characteristic curves of the LAM01+YSZ composite cathode cells at (a) 800, (b) 750, and (c) 700 °C. The cathode was baked at 1000 °C.

(a)

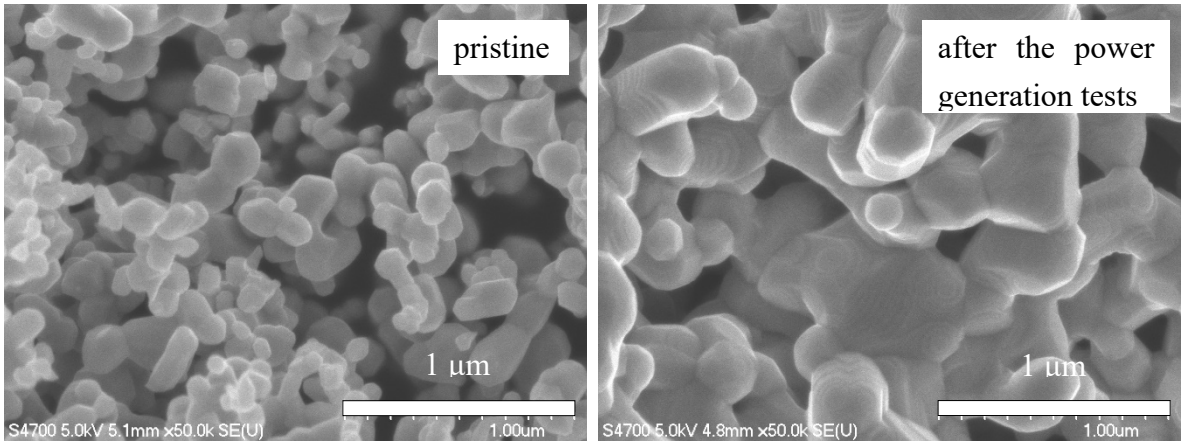

(b)

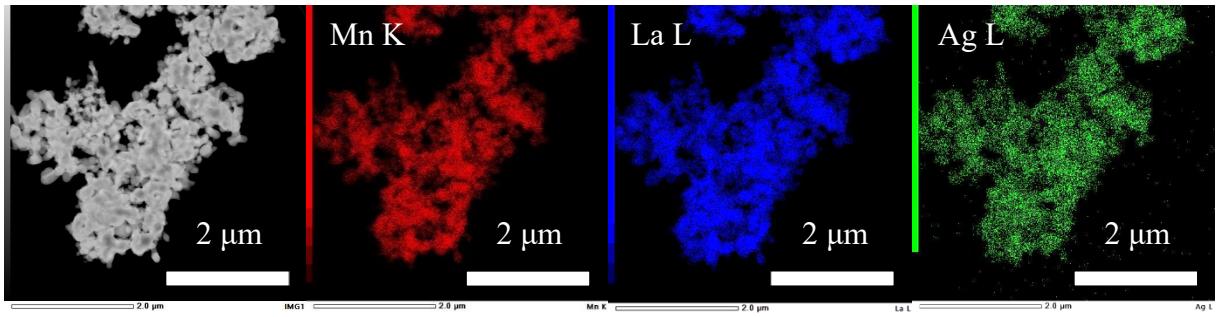

(c)

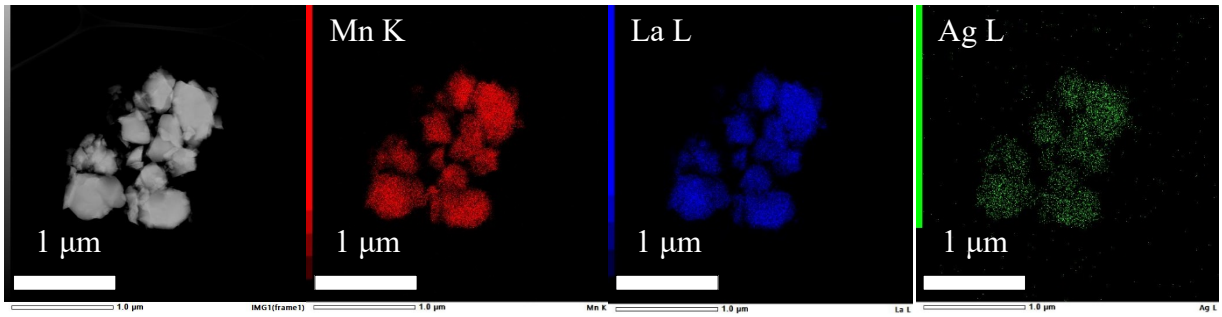

Figure S7 (a) SEM images of LAM01 powder before and after the power generation tests. HAADF-STEM images and elemental mapping by EDX of LAM01 (b) in the pristine state and (c) after the power generation tests. The cathode was baked at 1000 °C.

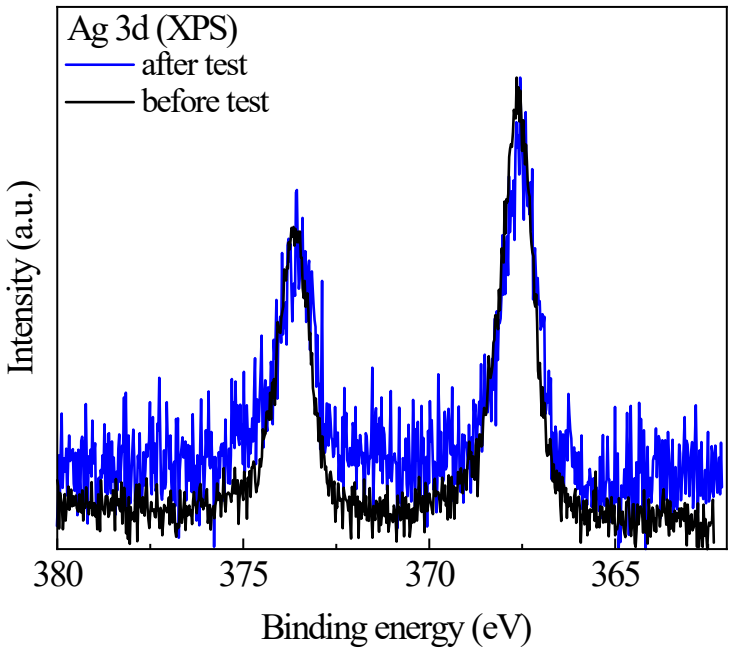

Figure S8 Ag 3d XPS spectra of LAM01 before and after the power generation tests. The cathode was baked at 1000 °C.

(a)

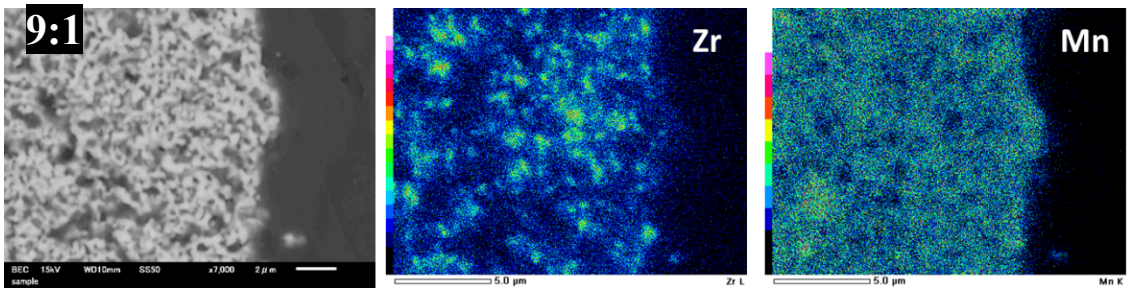

(b)

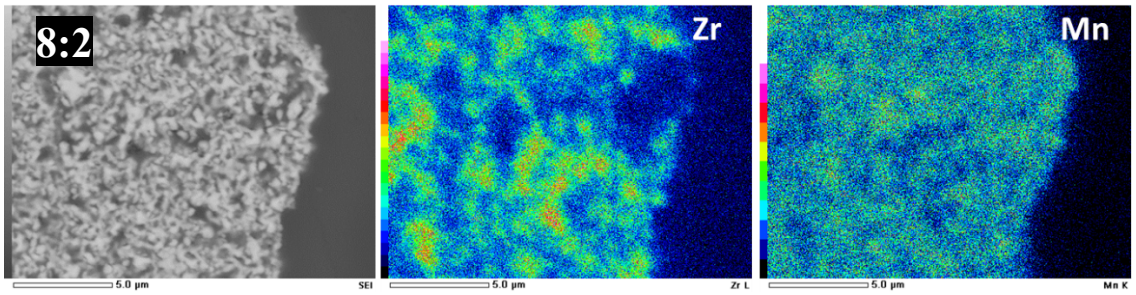

Figure S9 SEM images and EDX elemental mapping of the (a) LAM01+YSZ (9:1) composite cathode and (b) LAM01+YSZ (8:2) composite cathode after the power generation tests.

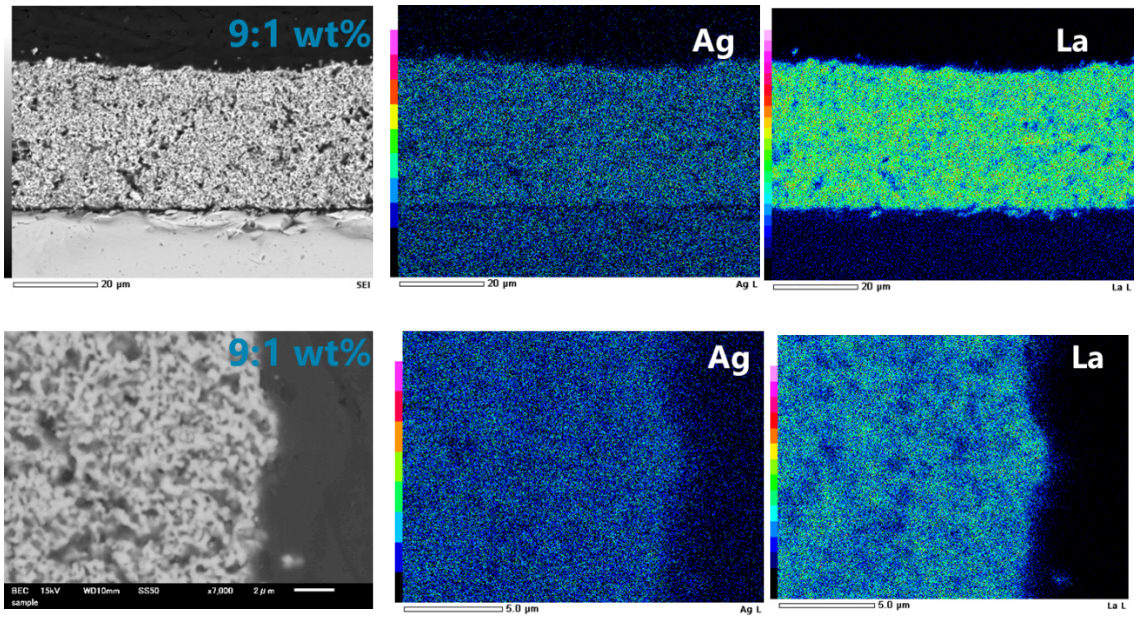

Figure S10 SEM images and EDX elemental mapping of Ag and La for the LAM01+YSZ (9:1) composite cathode cell after the power generation tests.

(a) (b)

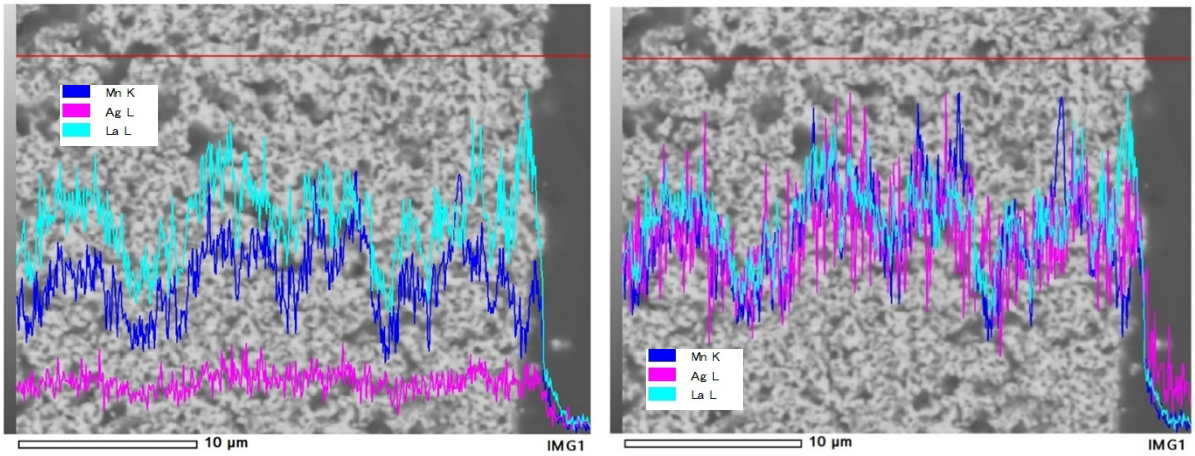

(c)

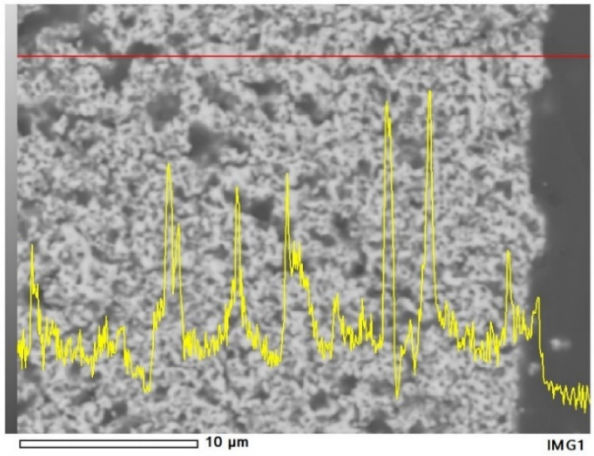

Figure S11 EDX elemental line scanning analysis of the LAM01+YSZ (9:1) composite cathode after the power generation tests. (a) La, Mn, and Ag line scanning profiles, (b) normalized La, Mn, and Ag line scanning profiles, and (c) Zr line scanning profile.

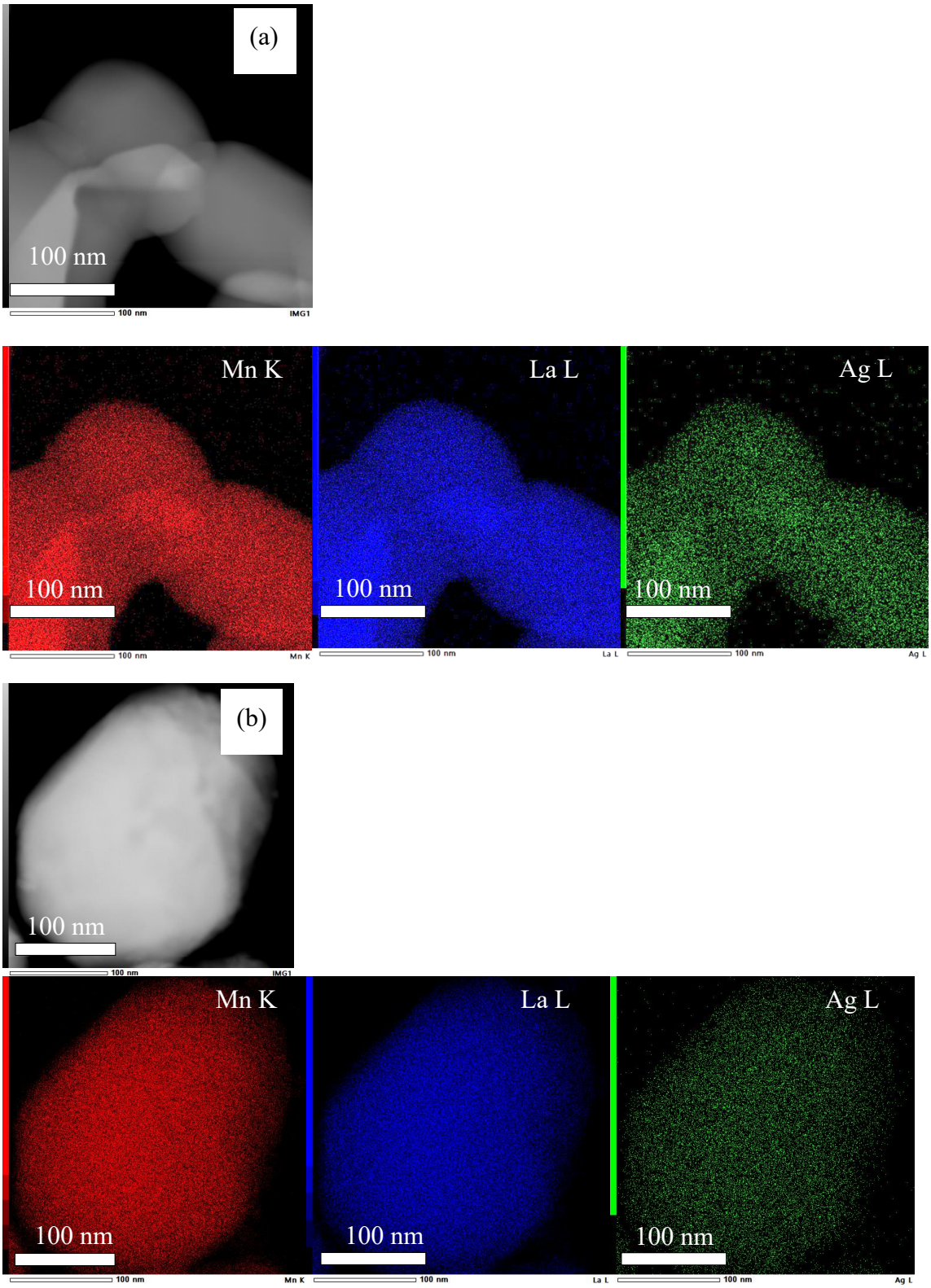

Figure S12 TEM images and EDX elemental mapping of the (a) LAM01 pristine powder and (b) LAM01 cathode (baked at 1000 °C) after the power generation tests.

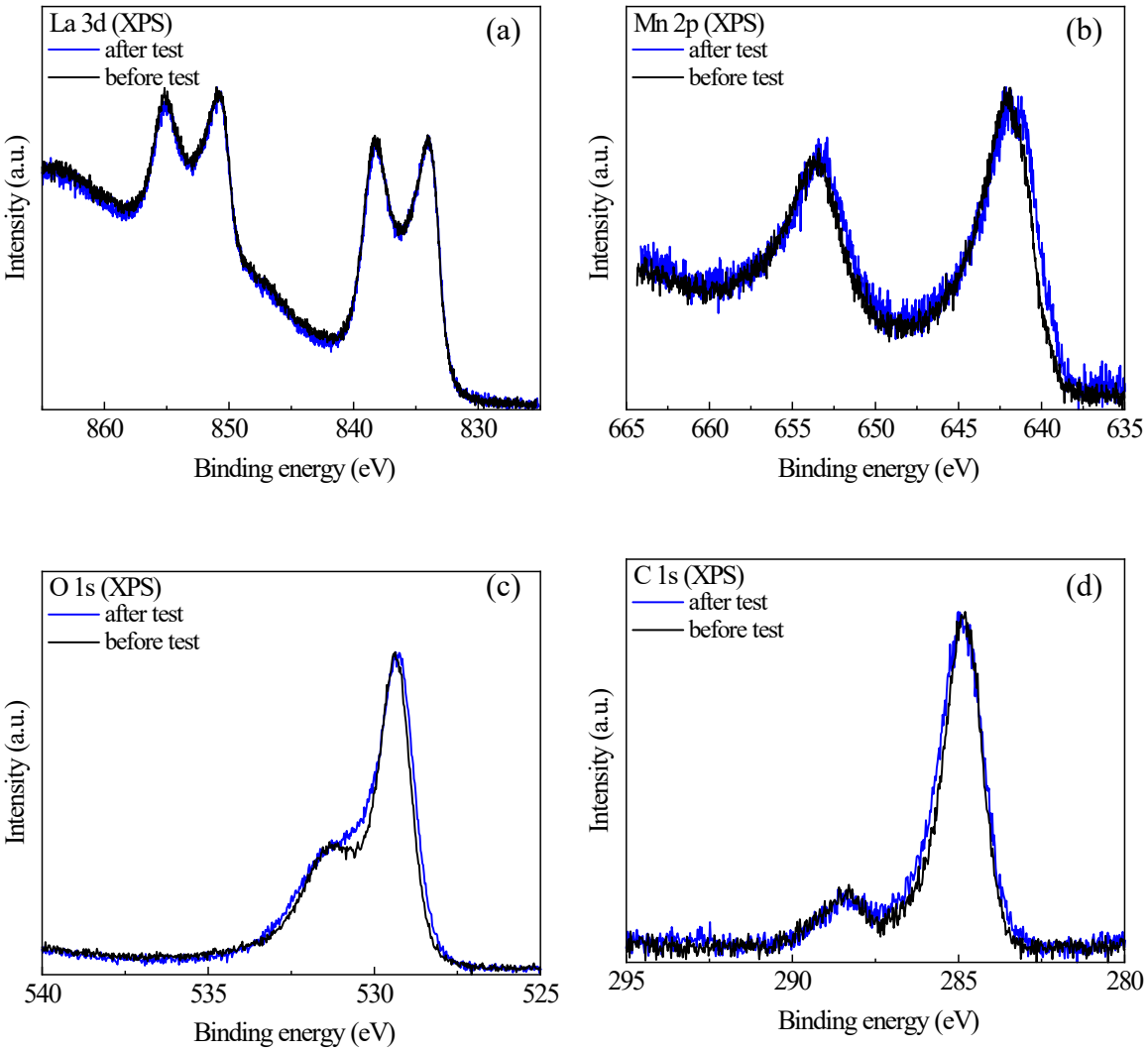

Figure S13 XPS spectra of pristine LAM01 powder and LAM01 cermet cathode after the power generation test. (a) La 3d, (b) Mn 2p, (c) O 1s, and (d) C 1s.

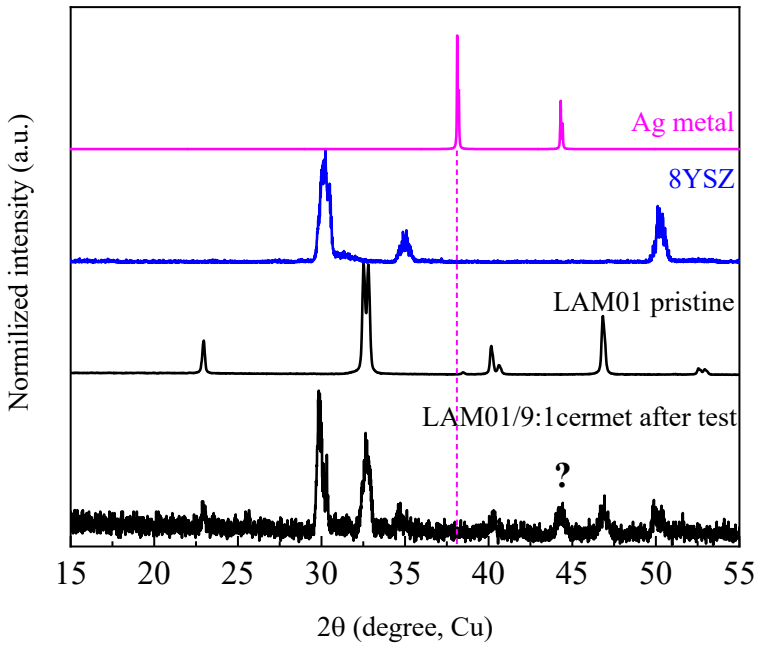

Figure S14 XRD profiles of the LAM01+YSZ (9:1) cermet cathode cell after the power generation tests. XRD was measured using parallel-beam X-rays (Smartlab, Rigaku Corp.).

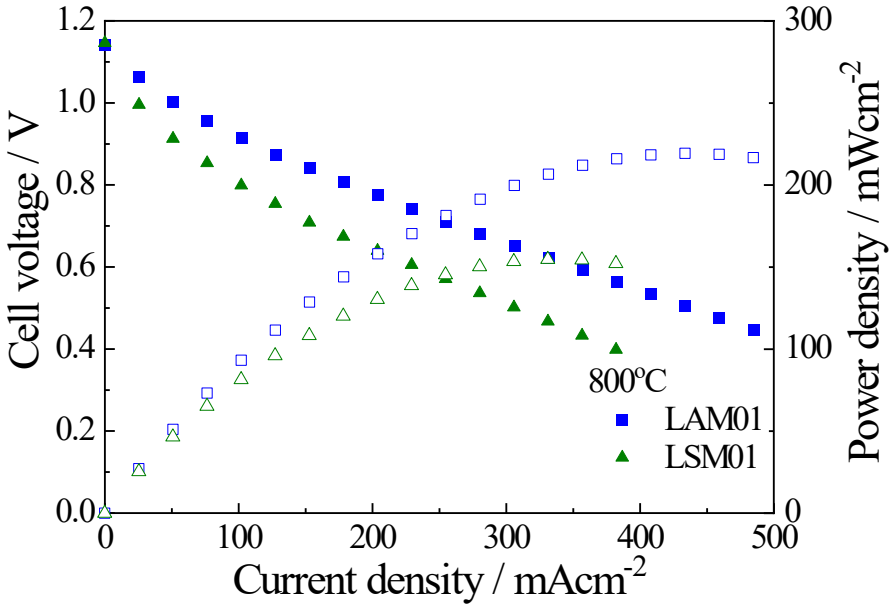

Figure S15 Comparison of power generation characteristic curves of the LAM01 cathode cell and LSM01 cathode cell at 800 °C. The cathodes were baked at 1000 °C.

Table S1 Crystal structure refinement by Rietveld analyses of pristine LAM01 and LAM02 powders.

Refined parameter	$La_{0.9}Ag_{0.1}MnO_3$	$La_{0.8}Ag_{0.2}MnO_3$
R_{wp} (%)	5.67	6.09
S	0.9635	1.5988
a, b (Å)	5.513	5.510
c (Å)	13.338	13.343
V (Å^3)	351.116	350.811

Table S2 EDX atomic concentrations obtained by SEM observation of pristine LAM01 powder, LAM01 powder annealed at 975 °C for 100 h, and the LAM01 cathode (baked at 925 and 1000 °C) after the power generation tests.

Pristine LAM01 powder (32 data points)

	Mn	Ag	La
Max. (at %)	51.1	4.8	54.4
Ave. (at %)	48.2	3.3	48.5
Min. (at %)	44.3	1.2	44.5

LAM01 powder annealed at 975 °C for 100 h (53 data points)

	Mn	Ag	La
Max. (at %)	58.4	4.3	57.3
Ave. (at %)	47.9	3.5	48.6
Min. (at %)	40.2	2.2	39.5

LAM01 cathode (baked at 925 °C) after the power generation tests (54 data points)

	Mn	Ag	La
Max. (at %)	49.5	3.5	53.3
Ave. (at %)	45.3	2.7	52.0
Min. (at %)	43.6	1.6	48.5

LAM01 cathode (baked at 1000 °C) after the power generation tests (35 data points)

	Mn	Ag	La
Max. (at %)	54.4	1.5	67.6
Ave. (at %)	49.6	0.7	49.7
Min. (at %)	32.4	0.0	44.7